Published in final edited form as:
Radiat Res. 2010 May ; 173(5): 579–589. doi:10.1667/RR2030.1.

Prevention and Mitigation of Acute Death of Mice after Abdominal Irradiation by the Antioxidant N-Acetyl-cysteine (NAC)

Dan Jia[1], **Nathan A. Koonce**, **Robert J. Griffin**, **Cassie Jackson**, and **Peter M. Corry**
Department of Radiation Oncology, University of Arkansas for Medical Sciences College of Medicine, Little Rock, Arkansas 72205

Abstract

Gastrointestinal (GI) injury is a major cause of acute death after total-body exposure to large doses of ionizing radiation, but the cellular and molecular explanations for GI death remain dubious. To address this issue, we developed a murine abdominal irradiation model. Mice were irradiated with a single dose of X rays to the abdomen, treated with daily s.c. injection of N-acetyl-L-cysteine (NAC) or vehicle for 7 days starting either 4 h before or 2 h after irradiation, and monitored for up to 30 days. Separately, mice from each group were assayed 6 days after irradiation for bone marrow reactive oxygen species (ROS), *ex vivo* colony formation of bone marrow stromal cells, and histological changes in the duodenum. Irradiation of the abdomen caused dose-dependent weight loss and mortality. Radiation-induced acute death was preceded not only by a massive loss of duodenal villi but also, surprisingly, abscopal suppression of stromal cells and elevation of ROS in the nonirradiated bone marrow. NAC diminished these radiation-induced changes and improved 10- and 30-day survival rates to >50% compared with <5% in vehicle-treated controls. Our data establish a central role for abscopal stimulation of bone marrow ROS in acute death in mice after abdominal irradiation.

INTRODUCTION

The abdomen is one of the body parts most vulnerable to radiation injury (1), and the gastrointestinal (GI) syndrome after a large dose of total-body or abdominal irradiation is one of the major causes of acute radiation lethality (2). Although this notion is supported by a close correlation between radiation death and loss of viable crypts in the intestine (3), it is far from all encompassing. Hematopoietic suppression has been demonstrated to occur concomitantly with GI injury and well before the occurrence of GI death in rodents (4), suggesting the possible contribution of bone marrow impairment to GI death. It has been known for more than 50 years that irradiation of one part of the body can elicit significant responses in remote, nonirradiated parts of the body (5–8), a phenomenon to which the term abscopal was assigned by Mole in 1953 (9). However, it remains unclear whether radiation injury to the GI tract triggers an abscopal suppression of bone marrow and whether such abscopal suppression, if existent, is involved in GI death.

At the molecular level, exposure to ionizing radiation is often followed by rapid elevation in inflammatory responses (10). The GI tract hosts the largest lymphoid tissue in the body, supporting the extra-thymic development and activation of T lymphocytes (11,12). A significant increase in the level of inflammatory cytokines such as TNF-alpha and IL-6 was

[1]Address for correspondence: Department of Radiation Oncology, University of Arkansas for Medical Sciences College of Medicine, 4301 W. Markham Street, Slot 824, Little Rock, AR 72205; JiaDan@uams.edu.

found in both the jejunum tissue and the peripheral blood in mice 3 days after abdominal X irradiation (13). The rationale of using anti-inflammatory treatment to mitigate radiation-induced tissue damage (10,14), although seemingly logical, has nonetheless been challenged. In an intriguing study, Wang *et al.* (15) found that deletion of the NFκB signaling upstream of a cascade of immune and inflammatory responses rendered mice more susceptible to intestinal radiation-induced acute death compared to wild-type controls. That study highlighted how little we know about the advantages and disadvantages of inflammatory responses and the optimal levels of these responses for tissue radioprotection and healing.

Several studies have shown extensive interactions between inflammatory responses and oxidative stress. Oxidative stress, often reflected by elevated levels of reactive oxygen species (ROS) and oxidation products, increases rapidly after radiation exposure (16–18), partially due to inflammation-stimulated generation of intracellular ROS (19). On the other hand, oxidative stress has been shown to activate redox-sensitive transcription factors such as AP-1 and NFκB, resulting in a new round of inflammatory cytokine production (20,21). In addition, ROS have been shown to activate macrophages and stimulate their tissue infiltration (22,23), a characteristic feature of inflammatory damage. Moreover, ROS blocks the negative-feedback control of the inflammatory process via suppression of inflammation-modulating molecules such as histone deacetylase 2 (HDAC-2) (23). The generation of inflammatory molecules and ROS after exposure to ionizing radiation therefore forms a vicious cycle, resulting in an inflammatory amplification. We postulated that controlling oxidative stress would be a way to limit radiation damage through pacing the initiation and subsequent amplification of inflammatory reactions.

In the present study, we used a mouse abdominal irradiation model to elicit lethality that is the consequence of acute GI injury without the interference of bone marrow suppression from direct radiation exposure of the skeleton. We report here on the role of abscopal stimulation of bone marrow ROS and suppression of bone marrow stromal cells in radiation-induced acute death.

MATERIALS AND METHODS

Mice

Male C57BL/6 mice were purchased from Harlan Laboratories (Indianapolis, IN) and given clean water and standard laboratory rodent chow (23.5% protein, 6.5% fat, 3.8% fiber, 6.8% ash, 3.3 kcal/g, 3.3 IU vitamin D3/g, 1.0% calcium, and 0.65% phosphorus, Formulab Diet 5008, LabDiet, St. Louis, MO) *ad libitum*. The mice were housed four or five per cage in plastic cages under standard laboratory conditions with a 12:12-h light/dark cycle, humidity of 48% and a constant temperature of 22°C. All procedures were approved by the UAMS Institutional Animal Care and Use Committee (IACUC).

Abdominal Irradiation

After an acclimatization period of 2 weeks, 10–12-week-old mice were individually tagged with an electronic identification chip (Bio Medic Data Systems, Inc., Seaford, DE) and randomized into sham and irradiated groups. A Faxitron X-ray Generating System (CP-160, Faxitron X-Ray Corp., Wheeling, IL) was used for all irradiations. Single-dose X rays were delivered at a dose rate of 1.079 Gy/min (150 kVp and 6.6 mA) to the abdomen of mice under sedation by i.p. injection of 100 mg/kg ketamine + 3 mg/kg xylazine. Abdominal exposure was achieved by shielding the non-abdominal body parts of the anesthetized mice placed on their right side using a customized cerrobend block (see Fig. 1 for illustration). The X-ray source-to-mid-abdomen distance was 50 cm, and the distance from the center of abdomen to the center of the plane was 26.7 cm. The radiation platform was rotated at 2 rpm during irradiation to

achieve uniform abdominal exposure. The mice were inspected twice a day and body weights were recorded daily for up to 30 days postirradiation. For separate experiments, animals were killed humanely 6 days after irradiation and tissues were collected for various assays (see below).

Radiation Dosimetry

Dosimetry was performed in a pilot study using a PTW Farmer Chamber (Model TN30013, Harpell Associates, Inc., Oakville, Ontario, Canada) connected to a CNMC Electrometer (CNMC Company Inc., Nashville, TN) following the TG-61 protocol. The absorbed dose rate was 1.079 Gy/min, calculated from the depth dose measurements taken with the chamber placed at the approximate mid-abdominal plane of a mouse positioned for irradiation.

NanoDot dosimeter chips (Landauer Corporate, Glenwood, IL) were used to verify the delivery of the targeted doses as well as shielding efficacy. The chips measured radiation exposure with aluminum oxide detectors read out by an InLight MicroStar® reader using optically stimulated luminescence (OSL) technology. The reader stimulates the detector with a light-emitting diode (LED) array, causing it to luminesce in proportion to the amount of radiation exposure. The luminescence is detected and measured by the reader's photomultiplier tube using a high-sensitivity photon counting system. A dose calculation algorithm is then applied to the measurement to determine exposure results. The wireless NanoDot dosimeters are small enough (i.e. 10 × 10 mm in dimension and 1 mm thick) to be placed simultaneously at multiple sites of a mouse body during a single radiation exposure. To determine the absorbed doses in the exposed abdomen, the NanoDot chips were placed at the center of the top surface of the abdomen of the mice positioned for irradiation. To determine shielding efficacy, the chips were placed at five sites of the mouse body positioned for a single-dose irradiation with 20 Gy, two at the exposed body sites (i.e., the top and bottom surfaces of the abdomen) and three at the shielded body sites (i.e., on top of chest, spine and thigh) (see Fig. 2).

N-Acetyl-cysteine (NAC) Treatment

Mice in each of the irradiated groups were further divided randomly into two subgroups. NAC (300 mg/kg body weight) or an equal volume of PBS was injected subcutaneously into the upper back of the mouse to circumvent the likely compromised GI absorption capacity after irradiation. Injections started either 4 h prior to (−4 h, prevention regimen) or 2 h after (+2 h, mitigation regimen) the beginning of irradiation and six subsequent daily injections were given over a total of 7 days. The NAC dose and injection method were based on published methods (24,25).

Complete Blood Cell Count

At 6 days after irradiation, whole blood was collected from mice by retro-orbital bleeding. Aliquots of whole blood were diluted with PBS. Complete blood cell counts were performed on a VetScan2 Blood Chemistry Analyzer (ABAXIS Inc., Union City, CA) following the instructions of the manufacturer.

Bone Marrow Harvest

After bleeding, the mice were killed by cervical dislocation. The tibiae and femurs were dissected and cleaned free of soft tissue with aseptic techniques. Bone marrow was flushed out of the long bones with α-MEM supplemented with 10% FBS and antibiotics. Bone marrow aspirates from the same mouse were pooled. Cells in the bone marrow aspirates were dispersed in the original flushing medium, passed through a 70-μm cell strainer, counted on a Z2 Coulter Counter, and processed immediately for *ex vivo* culture and measurement of reactive oxygen species (ROS).

Measurement of Bone Marrow ROS

Aliquots of bone marrow aspirates with equal number of cells were incubated with 2′,7′-dichlorofluorescein diacetate (DCFH-DA, Molecular Probes, Inc., Eugene, OR) to measure intracellular ROS (mainly H_2O_2) levels following the instructions of the manufacturer. The principle of the assay is that the non-ionic, non-polar DCFH-DA crosses cell membranes and is hydrolyzed by intracellular esterases to non-fluorescent DCFH. In the presence of ROS, DCFH is oxidized to form its highly fluorescent 2-electron oxidation product, 2′,7′-dichlorofluorescein (DCF) (26). Since the fluorescence intensity, measured at 485 nm (excitation)/530 nm (emission) on a fluorescence microplate reader (BioTek Instruments, Inc., Winooski, VT), is directly proportional to the concentration of hydrogen peroxide, the intracellular DCF fluorescence can be used to quantify the overall ROS in cells (27).

Ex Vivo Culture of Bone Marrow Cells

To generate fibroblast colony-forming units (CFU-F), a quantitative analysis of the numbers and proliferation capacities of mesenchyme-derived, undifferentiated progenitors of various non-hematopoietic lineages in the bone marrow that constitute part of the hematopoietic niche and are responsible for tissue repair (28,29), aliquots of bone marrow cell suspensions with equal number of cells were seeded in triplicate in 25-cm^2 flasks in α-MEM supplemented with antibiotics and 10% FBS. Medium was changed every 5 days, and the cultures were terminated when colonies of 50–100 fibroblast-like cells were formed. Cells were fixed in 10% neutral buffered formalin and stained with 0.1% methylene blue as described previously (30). The colonies were counted manually under a dissecting microscope.

Histology

At harvest, a 5-cm section of the duodenum was removed and fixed in 10% modified phosphate-buffered formalin (Surgipath, Richmond, IL) for 24–48 h. After fixation, the duodenum segments were embedded vertically in paraffin, cut into 5-μm cross sections, and stained with hematoxylin and eosin (H&E). The stained slides were scanned on a ScanScope XT System (Aperio Technologies, Inc., Vista, CA) and assessed qualitatively for villous shape, epithelial alignment and crypt abundance.

RESULTS

Establishment of a Mouse Model of Abdominal Irradiation

The shielding method used in the present study exposed approximately 15–20% of the mouse body mass (a large portion of the abdomen and small fraction of the lower chest) and less than 5% of the total skeleton (mainly portions of the unprotected ribs) to X rays. With the targeted doses ranging from 12.5 Gy to 20.0 Gy to be delivered to the mid-plane of the abdomen of the mice positioned for irradiation, the absorbed doses measured on the top surface of the mouse abdomen deviated less than 5.5% from the targeted doses (Fig. 2B). In a separate experiment in which the targeted dose was 20 Gy at the center of the exposed abdomen, the absorbed doses measured on the top and bottom surfaces of the exposed mouse abdomen were within 99.5 ± 7.5% and 91.0 ± 10.5% of the targeted dose, respectively (Fig. 2C). In contrast, the absorbed doses measured on the surface of the shielded thigh, chest and spine were 25.6 ± 8.9 cGy, 40.1 ± 5.1 cGy and 30.5 ± 2.9 cGy, respectively. Thus the estimated maximum radiation dose received by the shielded body parts (e.g. the skeleton) due to scatter and transmission did not exceed 50 cGy when the targeted doses to the abdomen did not exceed 20 Gy.

Dose-Dependent Body Weight Loss and Acute Death after Abdominal Irradiation

Body weight loss was evident in all irradiated mice, and it started as early as 1 day (24 h) after irradiation regardless of the radiation dose (Fig. 3A). Weight loss in mice exposed to 12.5 to

17.5 Gy peaked on days 5, 6, 6 and 7 after irradiation, respectively; surviving mice in these groups gradually regained their weight thereafter. Although the pace of earlier weight recovery was inversely related to radiation dose, the body weights of these mice all reached the preirradiation levels by day 22 after irradiation, and by day 30 the weights of these mice were comparable to those of the sham-irradiated mice (data not shown). In contrast, weight loss in mice exposed to 18.8 and 20.0 Gy continued until the animals died or were euthanized due to deteriorating health.

Parallel to the patterns of postirradiation weight loss was the radiation-induced acute mortality. With the exception of only one mouse in the 15-Gy group that died at day 5 postirradiation, all mice exposed to 12.5 and 15 Gy were alive on day 10 postirradiation (Fig. 3B). Mice exposed to higher doses, in contrast, started to die at postirradiation day 7, and the trend continued until day 10. All mice that survived the first 10 days after irradiation at these higher doses remained alive by day 30 (data not shown). We estimated an $LD_{50/D10}$ for abdominal irradiation of between 15 and 16 Gy, which is in line with an earlier study by Terry and Travis (31), who found the $LD_{50/D10}$ for total-abdominal irradiation in C3Hf/Kam mice was 15.6 Gy.

Small Intestinal Injury after Abdominal Irradiation

Figure 4 illustrates the histological features of H&E-stained cross sections of duodenal samples excised from mice 6 days after exposure to 0 and 20 Gy. Duodenum from sham-irradiated mice contained long and narrow mucosal villi that were tightly aligned and extended into the duodenum lumen. Each villus was enveloped by a layer of epithelial cells. The base of the villi was underlaid by numerous crypts, which form the regenerating zone of the villi. In contrast, the majority of the duodenal villi from mice exposed to 20 Gy appeared edematous. The alignment of the villi was distorted due to the shortened or destructed villi. Epithelial cells on the surface of the villi become disorganized, and the loss of crypts was evident. Exposure of mice to 50 cGy totalbody irradiation (TBI), a dose resembling the estimated maximum backscattered radiation from abdominal irradiation, did not cause detectable changes in duodenal histology at day 6 postirradiation (data not shown). This is consistent with the calculations by Terry and Travis showing that the D_0 for jejunal crypt death in C3Hf/Kam mice detected 3.5 days after TBI ranged between 0.96–1.31 Gy (31).

Suppression of Peripheral Leukocyte Counts and Bone Marrow Stromal Cells after Abdominal Irradiation

In addition to the damage to the small intestine directly exposed to X rays, 20 Gy of X rays caused an 80.1% decrease in total WBC counts in the peripheral blood 6 days after irradiation compared with cell counts from sham-irradiated mice, with a greater suppression seen in lymphocyte counts (Fig. 5A). Neither erythrocyte counts nor thrombocyte counts were altered by radiation at this time. Whether the differences in changes in cell counts imply a cell type-specific suppression of the hematopoietic populations by radiation or are merely the results of the varied life spans of these cells needs to be investigated further. Because bone marrow stroma is crucial for hematopoiesis, the decreased leukocyte count after abdominal irradiation could be secondary to bone marrow stromal cell suppression. To test this possibility, *ex vivo* bone marrow cultures were used to quantify the numbers and/or clonogenicity of bone marrow stromal cells isolated from nonirradiated tibiae and femurs 6 days after irradiation. Surprisingly, abdominal irradiation induced a 78.3% decrease in the number of fibroblast colony-forming units in *ex vivo* bone marrow culture compared with that in the sham-irradiated controls (Fig. 5B). There was no difference in colony size between the two samples, suggesting that the suppression was mainly due to the decline of the number of the stromal cells rather than to the loss of proliferation activity of these cells. To rule out the possibility that the suppression of bone marrow stroma after abdominal irradiation resulted from backscattered radiation, in a separate experiment, the same *ex vivo* assay was performed on bone marrow

from mice 6 days after TBI at 50 cGy, the estimated maximum scattered dose at the shielded skeletal sites of a mouse positioned for abdominal irradiation. No difference between bone marrow from the irradiated mice and sham-exposed controls was detected in the numbers and size of stromal colonies (data not shown). Therefore, suppression of bone marrow stroma by radiation is not a result of exposure to scattered radiation.

Elevation of ROS in Shielded Bone Marrow after Abdominal Irradiation

To elucidate the underlying mechanisms of radiation-induced abscopal suppression of hematopoiesis and the bone marrow stroma, we measured the level of ROS in the shielded bone marrow, because both ROS-induced hematopoietic suppression and bone marrow stroma impairment have been reported (32–34). A 3.8-fold increase in ROS levels was detected in the bone marrow 6 days after 20 Gy abdominal irradiation compared with that in the sham-irradiated mice (Fig. 5C). In contrast, bone marrow ROS levels were not altered in mice 6 days after 50 cGy TBI (data not shown), indicating that radiation-induced ROS spike in the shielded bone marrow was not due to scattered radiation.

Effects of NAC on Bone Marrow ROS Levels, Bone Marrow Stroma and Duodenum Histology after Abdominal Irradiation

To establish the role of ROS in radiation-induced tissue and cell damage, we used the non-specific antioxidant NAC to counteract elevation of ROS after irradiation. Mice subjected to sham exposure or a single dose of 20 Gy were also given an s.c. injection of NAC (300 mg/kg) or an equal volume of vehicle 4 h prior to irradiation followed by daily postirradiation injections. At day 6 after irradiation, bone marrow ROS levels in vehicle-treated mice increased by 4.8-fold compared with the sham-exposed counterparts (Fig. 6A). NAC treatment brought the ROS levels back to those of sham-exposed controls ($P > 0.05$ compared to 0 Gy; $P < 0.01$ compared to 20 Gy + vehicle). Conversely, the numbers of *ex vivo* bone marrow stromal colonies were greatly improved after NAC treatment compared with those in the vehicle-treated counterparts (Fig. 6B, $P > 0.05$ compared to 0 Gy; $P < 0.01$ compared to 20 Gy + vehicle). NAC treatment also preserved or restored the duodenal structure in mice exposed to 20 Gy and examined on day 6 after irradiation (Fig. 6C). Treatment of sham-exposed mice with NAC did not affect the baseline ROS levels in the bone marrow, *ex vivo* bone marrow stromal colony formation, or duodenal histological structure (data not shown).

NAC Treatment Prevented and Mitigated Radiation-Induced Acute Death in Mice

Weight loss occurred in mice exposed to 15 or 20 Gy (Fig. 7A). Daily NAC treatment for 7 days starting 4 h before irradiation (−4 h) did not affect the extent of weight loss in either irradiated group. In mice exposed to 15 Gy, NAC modestly improved the recovery of body weight starting on postirradiation day 5 ($P > 0.05$), and the body weights of both vehicle- and NAC-treated mice reached 105.7 ± 2.7% and 105.9 ± 4.7% of their preirradiation weights, respectively, by day 30 postirradiation. In mice exposed to 20 Gy, the body weight recovery of the survivors started 10 days after irradiation and reached 94.3 ± 0.3% and 93.6 ± 2.6% of the preirradiation weights by day 30 postirradiation for both vehicle- and NAC-treated groups, respectively. The body weight of sham-irradiated mice was not affected by NAC treatment.

NAC treatment had more profound effects on animal survival after lethal (i.e. 20 Gy) abdominal irradiation (Fig. 7B). The median survival time of the mice that died after 20 Gy was 8.5 days (7–10 days) in the vehicle-treated group and was increased to 9.5 days (9 and 10 days) after NAC treatment. More strikingly, both 10- and 30-day survival rates were increased to 68.8% after NAC treatment compared with <5% in the vehicle-treated counterparts.

To examine whether NAC could have a similar lifesaving impact when administered after exposing the mice to a lethal radiation dose (i.e. as a mitigation reagent), NAC was administered

2 h after 20 Gy (+2 h) followed by daily s.c. injection for a total of 7 days. Again, the 10- and 30-day survival rates were increased to 62.5% and 50%, respectively, in NAC-treated mice compared with <5% in the vehicle-treated controls (Fig. 7B).

DISCUSSION

In a nuclear incident, people who initially escape the instant death but are close to the epicenter are likely to fall victim to acute radiation sickness and die within days (GI death) or weeks (hematopoietic death) (35,36). GI death is attributed in general to irreversible GI injuries (3). Whether GI injury is the main cause of GI death, however, remains inconclusive, and the cellular and molecular mechanisms underlying GI death have been a subject of debate. Using a mouse model in which the interference of bone marrow suppression by direct exposure to ionizing radiation was minimized, we found that radiation-induced acute death was preceded not only by the destruction of the small intestine directly exposed to radiation but also by abscopal elevation of ROS and suppression of stromal cells in unirradiated bone marrow. Counteracting radiation-induced ROS with the nonspecific antioxidant NAC diminished the detrimental effects of radiation on bone marrow ROS level, bone marrow stromal cell numbers/viability, and duodenal structure. NAC both protected and rescued mice from lethal abdominal irradiation. Our findings demonstrate a causal relationship between abscopal stimulation of bone marrow oxidative stress and GI death after X irradiation of the abdomen in mice.

Many people exposed to intermediate to larger doses of radiation might be saved with immediate and effective medical care aimed at controlling the development of radiation injury. A major barrier to effective mitigation is the lack of identification of the lethal determinants of acute radiation death (i.e. GI death). Our results establish a central role for oxidative stress in radiation-induced acute death. These findings are consistent with reports by others showing the effectiveness of antioxidants in minimizing radiation-induced tissue damage in various animal models (37,38). Our demonstration of both radioprotection and mitigation by the common antioxidant NAC for lethal abdominal irradiation in mice suggests the possibility of developing effective mitigation strategies with the following features: greater efficacy in saving individuals exposed to lethal and sublethal radiation doses with few or no side effects on individuals exposed to lower doses, easy administration to the affected individuals, and wide availability.

NAC is a multifaceted non-specific small molecule antioxidant. In addition to its well-known role as the rate-limiting precursor of the natural free radical scavenger glutathione (39), NAC has also been found to possess catalase and glutathione reductase activities (40). Furthermore, cysteine has been shown to inhibit X-ray-induced hydroxyl radical generation in cell-free L-amino acid solutions (41). At present, we do not know how much each of these actions of NAC contributes to the beneficial effects observed in our animal model.

In the present study, ROS level was measured indirectly by quantifying the conversion of the non-fluorescent DCFH-DA to its fluorescent metabolite mainly by hydrogen peroxide. The increase in hydrogen peroxide in bone marrow after abdominal irradiation could result from some or all of the following: the increased production of hydroxyl radicals, exhaustion of the reduced form of glutathione, elevated conversion of superoxide to hydrogen peroxide, or suppressed decomposition of hydrogen peroxide. The mechanisms for induction of ROS by radiation are being investigated in ongoing studies in our laboratory. Since radiation-induced oxidative stress, both local and systemic, is likely to be long-lasting, we are also evaluating the long-term benefits of antioxidant therapy.

Crypt cells are sensitive to radiation injury, and GI death has been attributed to the loss of viable, regenerating crypts in the intestines (3). This notion, however, was contradictory to the

results of an earlier study by Terry and Travis (31), who found that at the $LD_{50/10}$, the number of jejunal crypts per jejunal circumference was an order of magnitude lower for mice surviving abdominal irradiation compared with that in mice given total-body irradiation (i.e. 5 and 65 crypts), suggesting that crypt loss by itself is not the major cause of radiation-induced GI mortality. In the present study, we detected not only the expected histological destruction of duodenum after lethal abdominal irradiation but also a pronounced abscopal suppression of stroma in unirradiated bone marrow. Our results demonstrate clearly a remote response to abdominal irradiation in the bone marrow. Since less than ≈5% of the mouse skeleton (mainly the unshielded ribs) was exposed to radiation in this model and since backscattered radiation did not cause detectable changes in either ROS levels in the bone marrow or the number/viability of bone marrow stromal cells, we infer that the suppression of bone marrow stroma must be caused by abscopal radiation effects, likely through the elevated ROS after higher doses of radiation. Although radiation-induced abscopal responses have been documented in the lungs of mice after abdominal irradiation (13), ours is the first to demonstrate the abscopal suppression of shielded bone marrow. While the results from our present study do not prove roles for either bone marrow stromal suppression in radiation-induced acute death or stromal preservation/rescue in the radioprotective effects of NAC, these two assumptions are supported by the following evidence.

First, bone marrow stromal cells are required for hematopoiesis in adult mammals to support the survival and self-renewal of the hematopoietic stem cells in a defined microenvironment in the bone marrow (also known as the hematopoietic niche) and inducing hematopoietic stem cell differentiation (42–45). Although ROS have been shown to suppress the proliferation and differentiation capacity of hematopoietic progenitors and induce apoptosis of mature cells of the hematopoietic lineage (32,33), the sharp decrease in leukocyte counts in the peripheral blood after abdominal irradiation, a sign of hematopoietic suppression, could also be secondary to the radiation-induced abscopal suppression of bone marrow stroma. Further investigation is needed to distinguish these two possible causes of hematopoietic suppression after irradiation and to identify the most susceptible cell types of the hematopoietic lineage. Since hematopoietic suppression is certainly a major causative factor of radiation-induced acute death (35,36), it is reasonable to postulate that radiation-induced acute death is attributable in part to abscopal myelosuppression. The existence of this unique form of myelosuppression is supported by *in vivo* findings by others showing that bone marrow hematopoietic shutdown in mice given 10 Gy TBI could be reversed by shielding the abdomen of the mice during irradiation (46). This early study and our present study together suggest the presence of at least two distinct hematopoietic populations, one sensitive to direct radiation exposure and the other more vulnerable to abscopal deprivation after abdominal irradiation. Preservation of the latter population might be essential for hematopoietic recovery from lethal doses of radiation.

Second, bone marrow stroma hosts the progenitors of virtually all mesenchymal lineages essential for tissue repair and regeneration (47–49). Earlier studies particularly relevant to our study demonstrated that bone marrow-derived cells contribute to epithelial repair in the GI tract of patients (50) and that infusion of mesenchymal stem cells accelerates intestinal recovery from radiation-induced destruction in mice (51). The improved duodenal structure in NAC-treated mice after abdominal irradiation as observed in the present study could have resulted from the migration of the preserved/rescued bone marrow stromal populations to the injured tissues (e.g. the gut). Alternatively, the improved duodenal structure at the time of examination could be due to a milder initial GI injury in the presence of NAC intervention. Further investigation will be aimed at quantifying the detrimental effects of abdominal irradiation on bone marrow stroma of various mesenchymal lineages and the impact of these effects on postirradiation tissue repair.

In summary, in the present study we established a causal link between the abscopal elevation of ROS in the unirradiated bone marrow and abdominal irradiation-induced acute death. The common non-specific antioxidant NAC was able to both prevent and mitigate radiation-induced acute death in mice. The increase in ROS levels in dying mice after abdominal irradiation was accompanied by abscopal suppression of bone marrow stroma; conversely, the normalization of ROS in mice saved by NAC was accompanied by the restoration of bone marrow stroma. Given the crucial roles for bone marrow stroma in both hematopoiesis and tissue repair, we postulate that the abscopal suppression of bone marrow stroma through the sharp increase in ROS is part of the cellular mechanism of abdominal irradiation-induced acute death in mice and that NAC protects/rescues mice from the acute death after abdominal irradiation through preserving/repopulating the bone marrow stromal cells. Preservation and/or revival of the bone marrow stroma sensitive to GI radiation injury might present a novel and effective way of mitigating radiation injury in a nuclear incident as well as in patients receiving significant doses of radiation in the abdominal area.

Acknowledgments

This work was funded by grants from the Department ofRadiation Oncology, University of Arkansas for Medical Sciences, by NIH Grant CA107160, and by the Kaufman's Foundation through Central Arkansas Radiation Therapy Institute (CARTI).

REFERENCES

1. Keefe DM, Gibson RJ, Hauer-Jensen M. Gastrointestinal mucositis. Semin. Oncol. Nurs 2004;20:38–47. [PubMed: 15038516]
2. Baverstock KF, Ash PJ. A review of radiation accidents involving whole body exposure and the relevance to the LD50/60 for man. Br. J. Radiol 1983;56:837–844. [PubMed: 6626874]
3. Hendry JH, Potten CS, Roberts NP. The gastrointestinal syndrome and mucosal clonogenic cells: relationships between target cell sensitivities, LD50 and cell survival, and their modification by antibiotics. Radiat. Res 1983;96:100–112. [PubMed: 6353474]
4. Mason KA, Withers HR, McBride WH, Davis CA, Smathers JB. Comparison of the gastrointestinal syndrome after total-body or total-abdominal irradiation. Radiat. Res 1989;117:480–488. [PubMed: 2648450]
5. Parsons WB Jr. Watkins CH, Pease GL, Childs DS Jr. Changes in sternal marrow following roentgen-ray therapy to the spleen in chronic granulocytic leukemia. Cancer 1954;7:179–189. [PubMed: 13126913]
6. Robin HI, AuBuchon J, Varanasi VR, Weinstein AB. The abscopal effect: demonstration in lymphomatous involvement of kidneys. Med. Pediatr. Oncol 1981;9:473–476. [PubMed: 7029238]
7. Petrovic N, Perovic J, Karanovic D, Todorovic L, Petrovic V. Abscopal effects of local fractionated X-irradiation of face and jaw region. Strahlentherapie 1982;158:40–42. [PubMed: 7058543]
8. Koturbash I, Rugo RE, Hendricks CA, Loree J, Thibault B, Kutanzi K, Pogribny I, Yanch JC, Engelward BP, Kovalchuk O. Irradiation induces DNA damage and modulates epigenetic effectors in distant bystander tissue *in vivo*. Oncogene 2006;25:4267–4275. [PubMed: 16532033]
9. Mole RH. Whole body irradiation; radiobiology or medicine? Br. J. Radiol 1953;26:234–241. [PubMed: 13042090]
10. Michalowski AS. Anti-inflammatory drug treatment of radiation injuries. Adv. Exp. Med. Biol 1997;400B:873–877. [PubMed: 9547641]
11. Abreu-Martin MT, Targan SR. Regulation of immune responses of the intestinal mucosa. Crit. Rev. Immunol 1996;16:277–309. [PubMed: 8922900]
12. Newberry RD, Lorenz RG. Organizing a mucosal defense. Immunol. Rev 2005;206:6–21. [PubMed: 16048539]
13. Van der Meeren A, Monti P, Vandamme M, Squiban C, Wysocki J, Griffiths N. Abdominal radiation exposure elicits inflammatory responses and abscopal effects in the lungs of mice. Radiat. Res 2005;163:144–152. [PubMed: 15658889]

14. Herodin F, Drouet M. Cytokine-based treatment of accidentally irradiated victims and new approaches. Exp. Hematol 2005;33:1071–1080. [PubMed: 16219528]
15. Wang Y, Meng A, Lang H, Brown SA, Konopa JL, Kindy MS, Schmiedt RA, Thompson JS, Zhou D. Activation of nuclear factor kappaB *in vivo* selectively protects the murine small intestine against ionizing radiation-induced damage. Cancer Res 2004;64:6240–6246. [PubMed: 15342410]
16. Biaglow JE, Ayene IS, Koch CJ, Donahue J, Stamato TD, Mieyal JJ, Tuttle SW. Radiation response of cells during altered protein thiol redox. Radiat. Res 2003;159:484–494. [PubMed: 12643793]
17. Avti PK, Pathak CM, Kumar S, Kaushik G, Kaushik T, Farooque A, Khanduja KL, Sharma SC. Low dose gammairradiation differentially modulates antioxidant defense in liver and lungs of Balb/c mice. Int. J. Radiat. Biol 2005;81:901–910. [PubMed: 16524845]
18. Hernandez-Flores G, Gomez-Contreras PC, Dominguez-Rodriguez JR, Lerma-Diaz JM, Ortiz-Lazareno PC, Cervantes-Munguia R, Sahagun-Flores JE, Orbach-Arbouys S, Scott-Algara D, Bravo-Cuellar A. Gamma-irradiation induced apoptosis in peritoneal macrophages by oxidative stress. Implications of antioxidants in caspase mitochondrial pathway. Anticancer Res 2005;25:4091–4100. [PubMed: 16309202]
19. Nagata M. Inflammatory cells and oxygen radicals. Curr. Drug Targets. Inflamm. Allergy 2005;4:503–504. [PubMed: 16101529]
20. Yao H, Yang SR, Kode A, Rajendrasozhan S, Caito S, Adenuga D, Henry R, Edirisinghe I, Rahman I. Redox regulation of lung inflammation: role of NADPH oxidase and NF-kappaB signalling. Biochem. Soc. Trans 2007;35:1151–1155. [PubMed: 17956299]
21. Rahman I, Biswas SK, Jimenez LA, Torres M, Forman HJ. Glutathione, stress responses, and redox signaling in lung inflammation. Antioxid. Redox Signal 2005;7:42–59. [PubMed: 15650395]
22. Cuschieri J, Maier RV. Oxidative stress, lipid rafts, and macrophage reprogramming. Antioxid. Redox Signal 2007;9:1485–1497. [PubMed: 17638545]
23. Kirkham P. Oxidative stress and macrophage function: a failure to resolve the inflammatory response. Biochem. Soc. Trans 2007;35:284–287. [PubMed: 17371261]
24. Zhang J, Dai J, Lu Y, Yao Z, O'Brien CA, Murtha JM, Qi W, Hall DE, Manolagas SC, Ershler WB. In vivo visualization of aging-associated gene transcription: evidence for free radical theory of aging. Exp. Gerontol 2004;39:239–247. [PubMed: 15036418]
25. Oliver SJ, Firestein GS, Arsenault L, Cruz TF, Cheng TP, Banquerigo ML, Boyle DL, Brahn E. Vanadate, an inhibitor of stromelysin and collagenase expression, suppresses collagen induced arthritis. J. Rheumatol 2007;34:1802–1809. [PubMed: 17696279]
26. LeBel CP, Ischiropoulos H, Bondy SC. Evaluation of the probe 2′,7′-dichlorofluorescin as an indicator of reactive oxygen species formation and oxidative stress. Chem. Res. Toxicol 1992;5:227–231. [PubMed: 1322737]
27. Wang H, Joseph JA. Quantifying cellular oxidative stress by dichlorofluorescein assay using microplate reader. Free Radic. Biol. Med 1999;27:612–616. [PubMed: 10490282]
28. Balduino A, Hurtado SP, Frazao P, Takiya CM, Alves LM, Nasciutti LE, El Cheikh MC, Borojevic R. Bone marrow subendosteal microenvironment harbours functionally distinct haemosupportive stromal cell populations. Cell Tissue Res 2005;319:255–266. [PubMed: 15578225]
29. Benayahu D, Akavia UD, Shur I. Differentiation of bone marrow stroma-derived mesenchymal cells. Curr. Med. Chem 2007;14:173–179. [PubMed: 17266576]
30. Jia D, Heersche JN. Insulin-like growth factor-1 and -2 stimulate osteoprogenitor proliferation and differentiation and adipocyte formation in cell populations derived from adult rat bone. Bone 2000;27:785–794. [PubMed: 11113389]
31. Terry NH, Travis EL. The influence of bone marrow depletion on intestinal radiation damage. Int. J. Radiat. Oncol. Biol. Phys 1989;17:569–573. [PubMed: 2528526]
32. Ito K, Hirao A, Arai F, Matsuoka S, Takubo K, Hamaguchi I, Nomiyama K, Hosokawa K, Sakurada K, Nakagata N, Suda T. Regulation of oxidative stress by ATM is required for self-renewal of haematopoietic stem cells. Nature 2004;431:997–1002. [PubMed: 15496926]
33. Ito K, Hirao A, Arai F, Takubo K, Matsuoka S, Miyamoto K, Ohmura M, Naka K, Hosokawa K, Ikeda Y, Suda T. Reactive oxygen species act through p38 MAPK to limit the lifespan of hematopoietic stem cells. Nat. Med 2006;12:446–451. [PubMed: 16565722]

34. Zhu H, Zhang L, Itoh K, Yamamoto M, Ross D, Trush MA, Zweier JL, Li Y. Nrf2 controls bone marrow stromal cell susceptibility to oxidative and electrophilic stress. Free Radic. Biol. Med 2006;41:132–143. [PubMed: 16781461]
35. Iijima S. Pathology of atomic bomb casualties. Acta Pathol. Jpn 1982;32(Suppl. 2):237–270. [PubMed: 7187578]
36. Okita T. Review of thirty years study of Hiroshima and Nagasaki atomic bomb survivors. II. Biological effects. A. Acute effects. J. Radiat. Res. (Tokyo) 1975;16(Suppl.):49–66. [PubMed: 1195203]
37. Rabbani ZN, Batinic-Haberle I, Anscher MS, Huang J, Day BJ, Alexander E, Dewhirst MW, Vujaskovic Z. Long-term administration of a small molecular weight catalytic metalloporphyrin antioxidant, AEOL 10150, protects lungs from radiation-induced injury. Int. J. Radiat. Oncol. Biol. Phys 2007;67:573–580. [PubMed: 17236973]
38. Parihar VK, Dhawan J, Kumar S, Manjula SN, Subramanian G, Unnikrishnan MK, Rao CM. Free radical scavenging and radioprotective activity of dehydrozingerone against whole body gamma irradiation in Swiss albino mice. Chem. Biol. Interact 2007;170:49–58. [PubMed: 17765885]
39. Lu SC. Regulation of hepatic glutathione synthesis: current concepts and controversies. FASEB J 1999;13:1169–1183. [PubMed: 10385608]
40. Aruoma OI, Halliwell B, Hoey BM, Butler J. The antioxidant action of N-acetylcysteine: its reaction with hydrogen peroxide, hydroxyl radical, superoxide, and hypochlorous acid. Free Radic. Biol. Med 1989;6:593–597. [PubMed: 2546864]
41. Shtarkman IN, Gudkov SV, Chernikov AV, Bruskov VI. Effect of amino acids on X-ray-induced hydrogen peroxide and hydroxyl radical formation in water and 8-oxoguanine in DNA. Biochemistry (Mosc.) 2008;73:470–478. [PubMed: 18457578]
42. Lord BI. The architecture of bone marrow cell populations. Int. J. Cell Cloning 1990;8:317–331. [PubMed: 2230283]
43. Mayani H, Guilbert LJ, Janowska-Wieczorek A. Biology of the hemopoietic microenvironment. Eur. J. Haematol 1992;49:225–233. [PubMed: 1473584]
44. Arai F, Suda T. Maintenance of quiescent hematopoietic stem cells in the osteoblastic niche. Ann. NY Acad. Sci 2007;1106:41–53. [PubMed: 17332071]
45. Han W, Yu Y, Liu XY. Local signals in stem cell-based bone marrow regeneration. Cell Res 2006;16:189–195. [PubMed: 16474433]
46. Vavrova J, Petyrek P. Shielding of the abdominal region during X-irradiation: effect on haemopoietic stem cells. Folia Biol. (Praha) 1984;30:267–275. [PubMed: 6479369]
47. Takahashi T, Kalka C, Masuda H, Chen D, Silver M, Kearney M, Magner M, Isner JM, Asahara T. Ischemia- and cytokine-induced mobilization of bone marrow-derived endothelial progenitor cells for neovascularization. Nat. Med 1999;5:434–438. [PubMed: 10202935]
48. Orlic D, Kajstura J, Chimenti S, Jakoniuk I, Anderson SM, Li B, Pickel J, McKay R, Nadal-Ginard B, Bodine DM, Anversa P. Bone marrow cells regenerate infarcted myocardium. Nature 2001;410:701–705. [PubMed: 11287958]
49. Shimizu K, Sugiyama S, Aikawa M, Fukumoto Y, Rabkin E, Libby P, Mitchell RN. Host bone-marrow cells are a source of donor intimal smooth-muscle-like cells in murine aortic transplant arteriopathy. Nat. Med 2001;7:738–741. [PubMed: 11385513]
50. Okamoto R, Yajima T, Yamazaki M, Kanai T, Mukai M, Okamoto S, Ikeda Y, Hibi T, Inazawa J, Watanabe M. Damaged epithelia regenerated by bone marrow-derived cells in the human gastrointestinal tract. Nat. Med 2002;8:1011–1017. [PubMed: 12195435]
51. Semont A, Francois S, Mouiseddine M, Francois A, Sache A, Frick J, Thierry D, Chapel A. Mesenchymal stem cells increase self-renewal of small intestinal epithelium and accelerate structural recovery after radiation injury. Adv. Exp. Med. Biol 2006;585:19–30. [PubMed: 17120774]

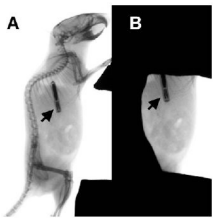

FIG. 1.

Mouse abdominal irradiation model. Radiographs of (panel A) an unshielded 10-week-old male C57BL/6 mouse with an electronic transponder (arrow) implanted subcutaneously in the upper right back and (panel B) the same mouse positioned for abdominal irradiation with the skeleton shielded by an investigator-designed cerrobend block. Radiography was taken using a Kodak *In Vivo* Fx Optical Imaging System (Carestream Health, Inc., Rochester, NY).

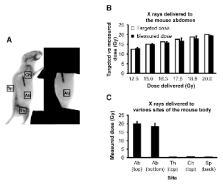

FIG. 2.

Verification of absorbed doses at the abdomen and validation of shielding efficacy. Ten-week-old male C57BL/6 mice under anesthesia were positioned for irradiation. After dosimetry performed using a PTW Farmer Chamber connected to a CNMC Electrometer that was positioned at the approximated mid-abdomen position, absorbed doses of X rays of various targeted doses at multiple body parts of a mouse were measured using the NanoDot dosimeter chips. Panel A: Positioning of the NanoDot dosimeter chips in a mouse exposed to radiation. NanoDot dosimeter chips were placed on the center of the top and bottom surface of the exposed abdomen (Ab) as well as on the top of the shielded left thigh (Th), chest wall (Ch) and spine (Sp) of anesthetized mice. The mouse was then exposed to 12.5–20.0 Gy X rays at a dose rate of 1.079 Gy/min using a Faxitron X-ray Generating System (CP-160, Faxitron X-Ray Corp., Wheeling, IL). Panel B: Comparison of targeted doses and absorbed doses measured on the top surface of the exposed mouse abdomen positioned for irradiation. Bars are the means and standard deviations calculated from readings on five mice, one reading per dose per mouse. Panel C: Absorbed doses measured at various sites of the mouse body positioned for irradiation. Data are the means and standard deviations calculated from readings on two mice with three readings per site per mouse.

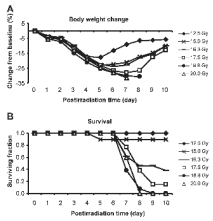

FIG. 3.

Weight loss and surviving fraction after abdominal irradiation. Panel A: Postirradiation changes in body weight. Weight loss is expressed as percentage difference from baseline body weight recorded immediately prior to irradiation. Data are the means of the percentage weight changes. Standard deviations of the means, which ranged from 0.2 to 6.7, are omitted from the graph for simplicity. n = 5–13 per dose. Panel B: Surviving fraction at day 10 (n = 5–13).

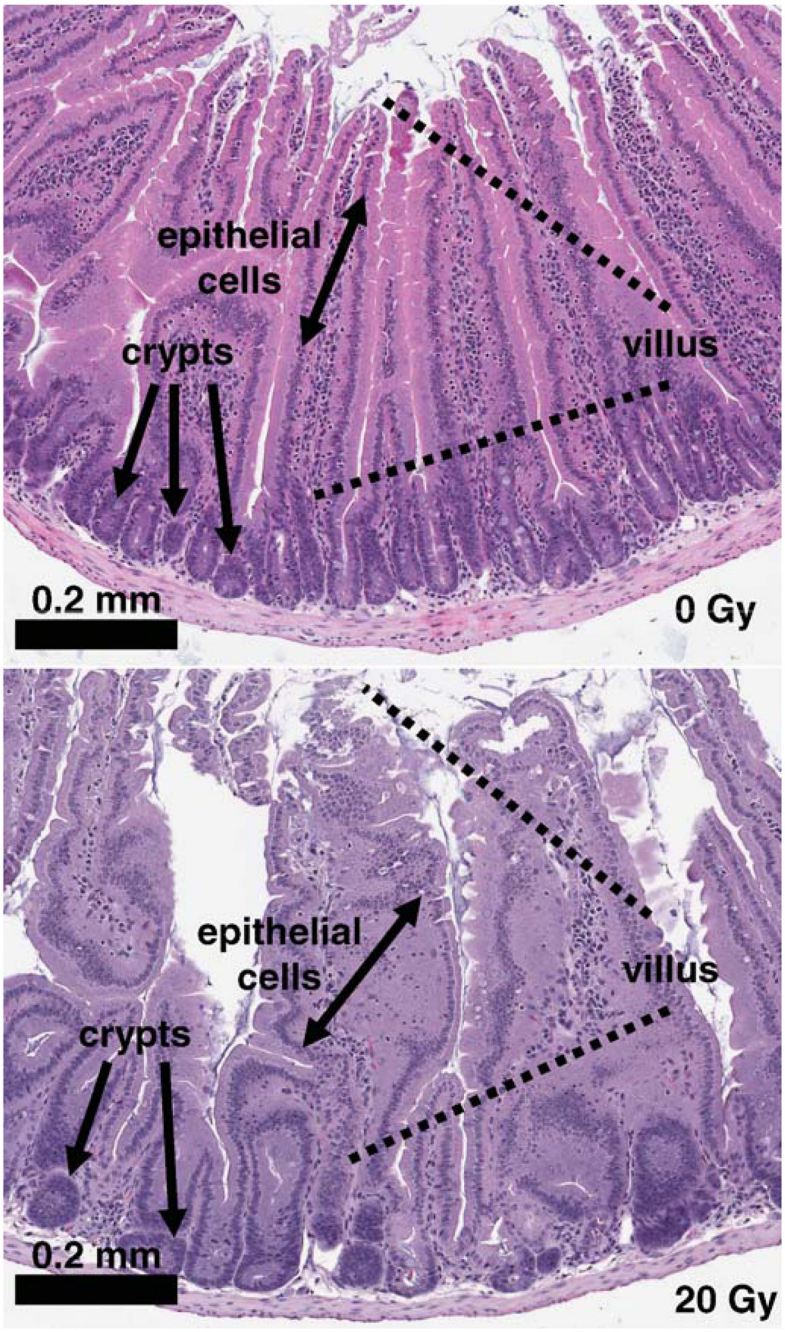

FIG. 4.
Histology of small intestine after abdominal irradiation. Representative images from three mice per group; two or three slides per mouse are shown. Scale bar: 0.2 mm.

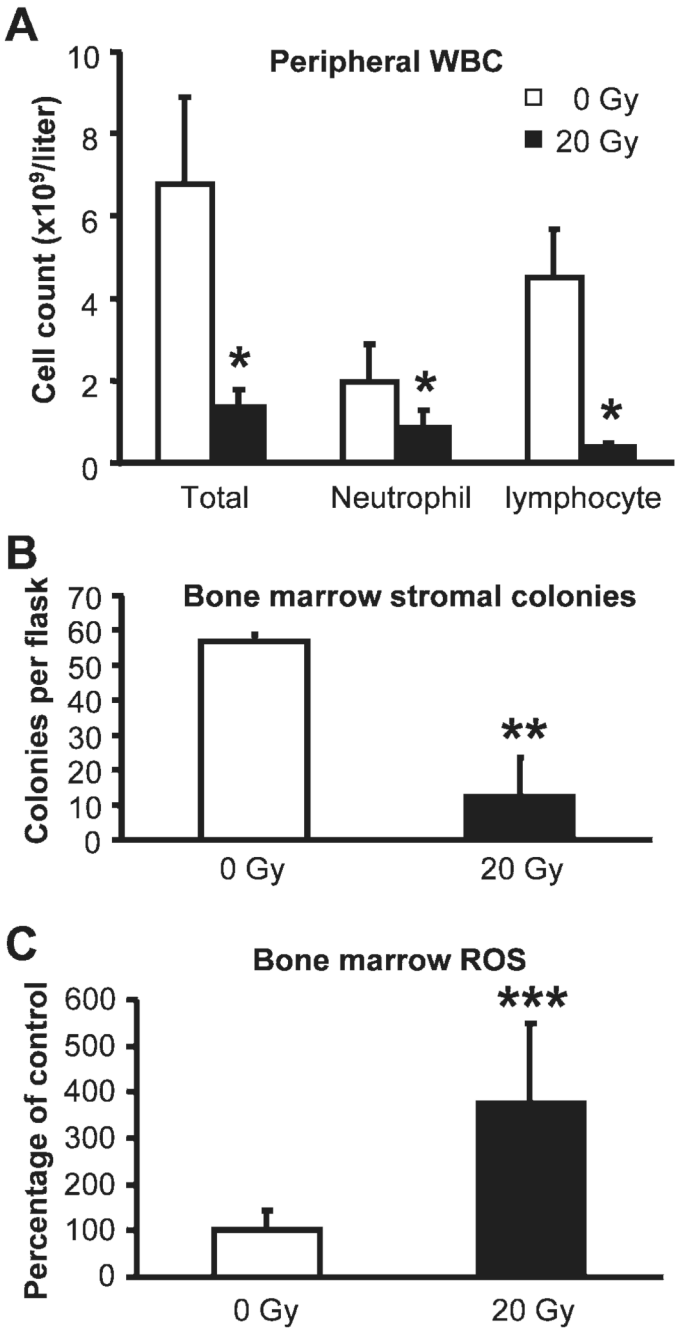

FIG. 5.

Peripheral white blood cell counts (panel A), *ex vivo* bone marrow stromal colony formation (panel B), and bone marrow ROS measurements (panel C) 6 days after abdominal irradiation. ROS measurements were normalized to cell number and expressed as percentages of the levels in the controls. Data are means and standard deviations. *$P < 0.001$ ($n = 10–12$); **$P < 0.01$ ($n = 3$); ***$P < 0.01$ ($n = 8$).

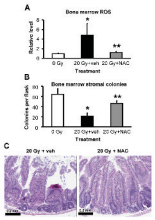

FIG. 6.

Effects of NAC treatment on bone marrow ROS levels, *ex vivo* stromal colony formation and duodenum histology in mice exposed to abdominal irradiation. ROS levels (panel A) and *ex vivo* fibroblast colony-forming unit formation (panel B) in bone marrow were quantified as described in the Materials and Methods. ROS measurements were normalized to cell numbers and expressed as percentage of the levels in the controls. Data are means and standard deviations (n = 3–4 mice per group). *P <0.01 compared to 0 Gy, **P <0.05 compared to 20 Gy + veh. Panel C: Histological features of duodenum 6 days after abdominal irradiation. Photographs are representative of images from three or four mice per group, two or three slides per mouse. Scale bar: 0.2 mm.

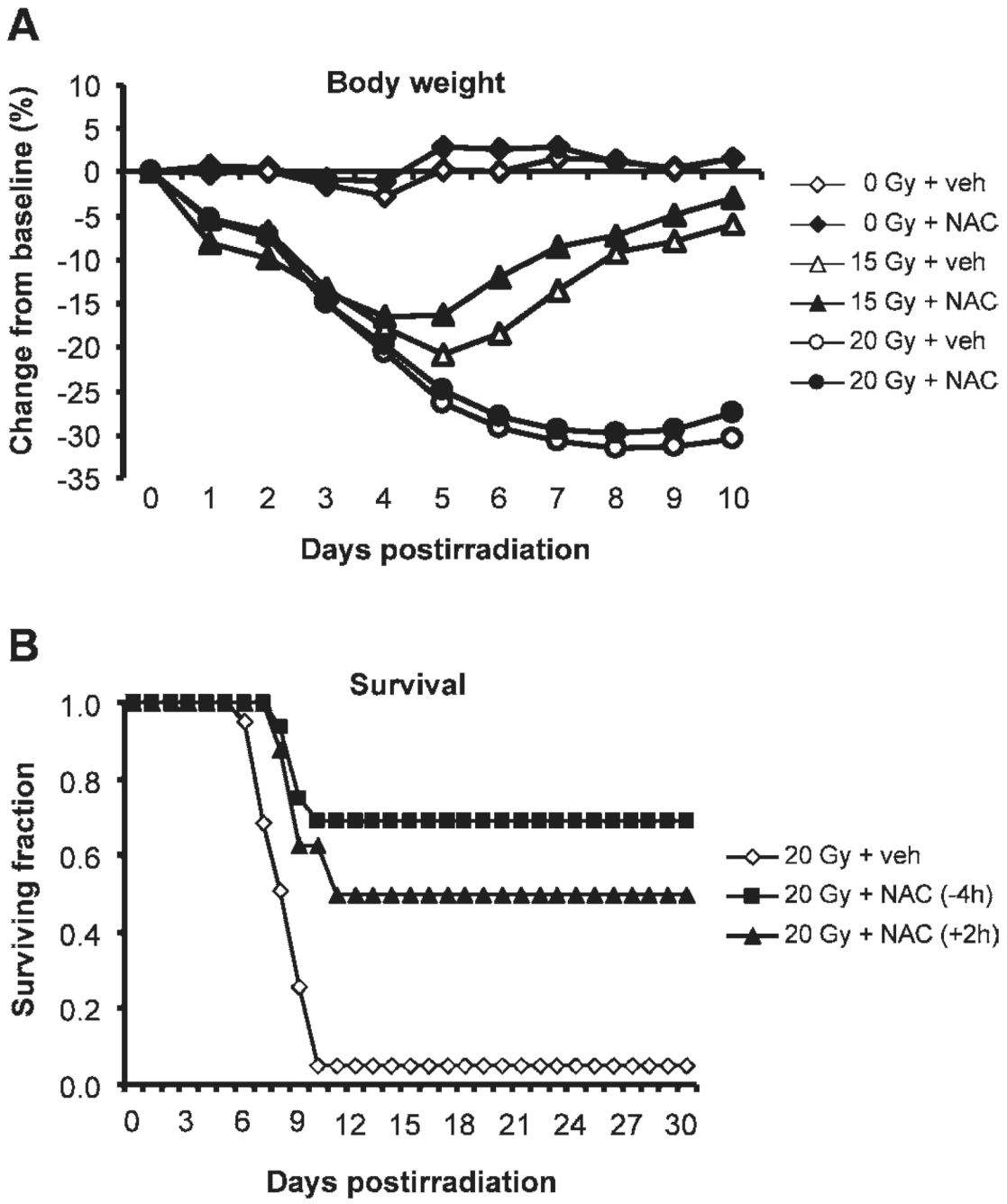

FIG. 7.

Effects of NAC treatment on body weight and survival after abdominal irradiation. Panel A: Postirradiation changes in body weight. Data are the means of the percentage change in body weight from the baseline. Standard deviations of the means, which ranged from 0.9 to 6.7, are omitted from the graph for simplicity (n = 16–41). Panel B: Postirradiation surviving fractions. Calculated from data pooled from five experiments (n = 16–41).